Translational Oncology
www.transonc.com

Volume 12 Number 2 February 2019 pp. 226–235 226

Multi-Spectral Fluorescence Imaging of Colon Dysplasia *In Vivo* Using a Multi-Spectral Endoscopy System[1]

Sang Mun Bae[*,†], Dong-Jun Bae[*], Eun-Ju Do[*], Gyungseok Oh[‡], Su Woong Yoo[§], Gil-Je Lee[¶], Ji Soo Chae[¶], Youngkuk Yun[¶], Sungjee Kim[#], Ki Hean Kim[**], Euiheon Chung[‡,§], Jun Ki Kim[††], Sung Wook Hwang[‡‡], Sang Hyoung Park[‡‡], Dong-Hoon Yang[‡‡], Byong Duk Ye[‡‡], Jeong-Sik Byeon[‡‡], Suk-Kyun Yang[‡‡], Jinmyoung Joo[††,§§], Sang-Yeob Kim[*,§§] and Seung-Jae Myung[*,‡‡,§§]

[*]Asan Institute for Life Sciences, Asan Medical Center, University of Ulsan College of Medicine, Seoul 138-736, South Korea; [†]Department of Medicine, University of Ulsan College of Medicine, Seoul 138-736, South Korea; [‡]School of Mechanical Engineering, Gwangju Institute of Science and Technology, Gwangju 61005, South Korea; [§]Department of Biomedical Science and Engineering, Institute of Integrated Technology (IIT), Gwangju, Institute of Science and Technology, Gwangju 61005, South Korea; [¶]Discovery and Analytic Solution, PerkinElmer Korea, Seoul 08380, South Korea; [#]Department of Chemistry, Pohang University of Science and Technology, Pohang 790-784, South Korea; [**]Department of Mechanical Engineering, Pohang University of Science and Technology, Pohang 790-784, South Korea; [††]Biomedical Engineering Research Center, Asan Institute for Life Sciences, Asan Medical Center, University of Ulsan College of Medicine, Seoul 138-736, South Korea; [‡‡]Department of Gastroenterology, Asan Medical Center, University of Ulsan College of Medicine, Seoul 138-736, South Korea; [§§]Department of Gastroenterology and Convergence Medicine, University of Ulsan College of Medicine, Seoul 138-736, South Korea

Abstract

BACKGROUND AND STUDY AIM: To develop a molecular imaging endoscopic system that eliminates tissue autofluorescence and distinguishes multiple fluorescent markers specifically on the cancerous lesions. *METHODS:* Newly developed multi-spectral fluorescence endoscope device has the potential to eliminate signal interference due to autofluorescence and multiplex fluorophores in fluorescent probes. The multiplexing capability of the multi-spectral endoscope device was demonstrated in the phantom studies and multi-spectral imaging with endoscopy and macroscopy was performed to analyze fluorescence signals after administration of fluorescent probe that targets cancer in the colon. Because of the limitations in the clinical application using rigid-type small animal endoscope, we developed a flexible channel insert-type fluorescence endoscope, which was validated on

Address all correspondence to: Sang-Yeob Kim, Asan Institute for Life Sciences, Asan Medical Center, University of Ulsan College of Medicine, Seoul 138-736, South Korea. E-mail: sjmyung@amc.seoul.kr or Seung-Jae Myung, Department of Convergence Medicine, University of Ulsan College of Medicine, Seoul 138-736, South Korea.
E-mail: sykim3yk@amc.seoul.kr

[1] Funding: This research was supported by the grant of the Korea Health Technology R&D Project through the Korea Health Industry Development Institute(KHIDI), funded by the Ministry of Health & Welfare, Republic of Korea. (No. HI15C3078), and the grant supported by the Ministry of Trade, Industry & Energy (MOTIE, Korea) under Industrial Technology Innovation Program. (No. 10063408), and the grant from Asan Institute for Life Sciences (No. 2015–7008).
Received 15 June 2018; Revised 7 October 2018; Accepted 11 October 2018

1936-5233/19
https://doi.org/10.1016/j.tranon.2018.10.006

the colonoscopy of dummy and porcine model. *RESULTS:* We measured multiple fluorescent signals simultaneously, and the fluorescence spectra were unmixed to separate the fluorescent signals of each probe, in which multiple fluorescent probes clearly revealed spectral deconvolution at the specific targeting area in the mouse colon. The positive area of fluorescence signal for each probe over the whole polyp was segmented with analyzing software, and showed distinctive patterns and significantly distinguishable values: 0.46 ± 0.04, 0.39 ± 0.08 and 0.73 ± 0.12 for HMRG, CET-553 and TRA-675 probes, respectively. The spectral unmixing was finally demonstrated in the dummy and porcine model, corroborating the targeted multi-spectral fluorescence imaging of colon dysplasia. *CONCLUSION:* The multi-spectral endoscopy system may allow endoscopists to clearly identify cancerous lesion that has different patterns of various target expression using multiple fluorescent probes.

Translational Oncology (2019) 12, 226–235

Introduction

Colorectal cancer is one of the most common cancer diagnosed, and has been the second leading cause of cancer death [1]. Early detection of colorectal cancer can prevent cancer progression and increase chances of survival. Screening colonoscopy aided by white light illumination currently performed for early detection to identify and remove polypoid adenomas for preventing cancer development and progression [2,3]. However, some malignant polyps are flat in architecture and patchily distributed, resulting in limited detection of early stage tumors in patient undergoing adenoma-carcinoma sequence [4,5]. Distinguishing the changes between the normal and dysplastic tissue depends thoroughly on the expertise of endoscopists, thus it is hampered by empirical decision on obscure lesions that are hardly discriminative by naked eye [6,7].

The significant problem to detect true signal spectra of 'smart' molecular reagents labeled with fluorophore *in vivo* is that the spectra are always admixed with autofluorescence signals [8,9]. There are two major methods to remove tissue autofluorescence in *in vivo* imaging: utilizing fluorescence lifetime information and removing tissue autofluorescence is by using multispectral imaging (MSI). The former is needed expensive pulsed lasers and the latter has lower cost and higher speed than the former [9].

Recent advances in gastrointestinal endoscopy have resulted in new imaging methods that improve the detection capability of early neoplastic lesions [10–12], such as narrowband and autofluorescence imaging, nonspecific contrast mechanisms are still challenging.

Potential uses of fluorescent agents have been demonstrated to monitor molecular changes [13] and therefore visualize molecular changes specific for colorectal cancer *in vivo* and, as a result, indicate a distinguishable region [14,15]. Multiple probes enable specific targeting and verification of the cancer-related cellular changes, and further confer reliable assurance for cancer diagnosis. The fluorescent signals of each targeting probe is typically measured and analyzed by multi-spectral imaging devices, and recently equipped with endoscopy system [8,10,14–19]. However, conventional imaging systems suffer from limited sensitivity to fluorescent spectral overlap and deconvolution [19].

Here we introduce a home-built instrument for multi-fluorescent imaging and demonstrate the capability of spectral unmixing with various fluorophore dyes. The multi-spectral endoscopy system is equipped with a liquid crystal tunable filter (LCTF), in which multiple fluorophores that have spectral overlap can be sharply separated by using multiband acquisition [20]. Moreover, LCTF excludes tissue autofluorescence, thus improves contrast by decreasing target-to-background ratio to make the inspected target clearly discriminated [9,21]. It has been widely reported that EGFR [22–26] and HER2 are abundantly expressed in the tumor, thus the antibodies that are labeled with fluorescent dyes become fluorescent probe for detection of these receptors [27–29]. The integrated imaging system is then validated to visualize individual dysplasia in a colon cancer mouse model with administration of multiple fluorescent probes that target the polyps. To measure and quantify the effective fluorescence signal, which eliminated background and autofluorescence by unmixing, the signal of each probe was subjected to threshold segmentation through inform software (PerkinElmer, Hopkinton, MA). Finally, we combined the multi-spectral imaging system to channel insert-type endoscope, and performed the colonoscopy in the porcine model to verify the potential clinical application.

Methods

Multi-Spectral Fluorescence and White Light Imaging Endoscope System

The imaging system is composed of a 0°cysto-urethroscope (Karl Storz, Tuttlingen, Germany), multi-spectral imaging system (Nuance FX, PerkinElmer, Hopkinton, MA), sensitive color charge-coupled device (CCD) camera (QIClick, QImaging, Surrey, BC, Canada), and achromatic lenses as depicted Figure 1*A*. A rigid type cysto-urethroscope probe (HOPKINS II Telescope 27301AA, Karl Storz, Tuttlingen, Germany) is coupled to both cameras *via* the beam splitter, which functions as channels for white light and fluorescent excitation source. Singlet lens collimate the light to the cameras, and the light transmits to both CCD detector in the camera and the Nuance camera (1392 × 1040 pixels). The excitation energy is generated by 300-W Xenon lamp (MAX-303, Asahi Spectra, Torrance, CA) with band-pass filters (480/30 nm, 540/25 nm and 679/41 nm) that excites fluorophores of corresponding fluorescent probes.

The Nuance Imaging Module was built in a single compact package containing the principal imaging components: scientific-grade CCD imaging sensor, liquid crystal tunable filter (LCTF) which has a scanning range between 420 and 720 nm with a polarizer,

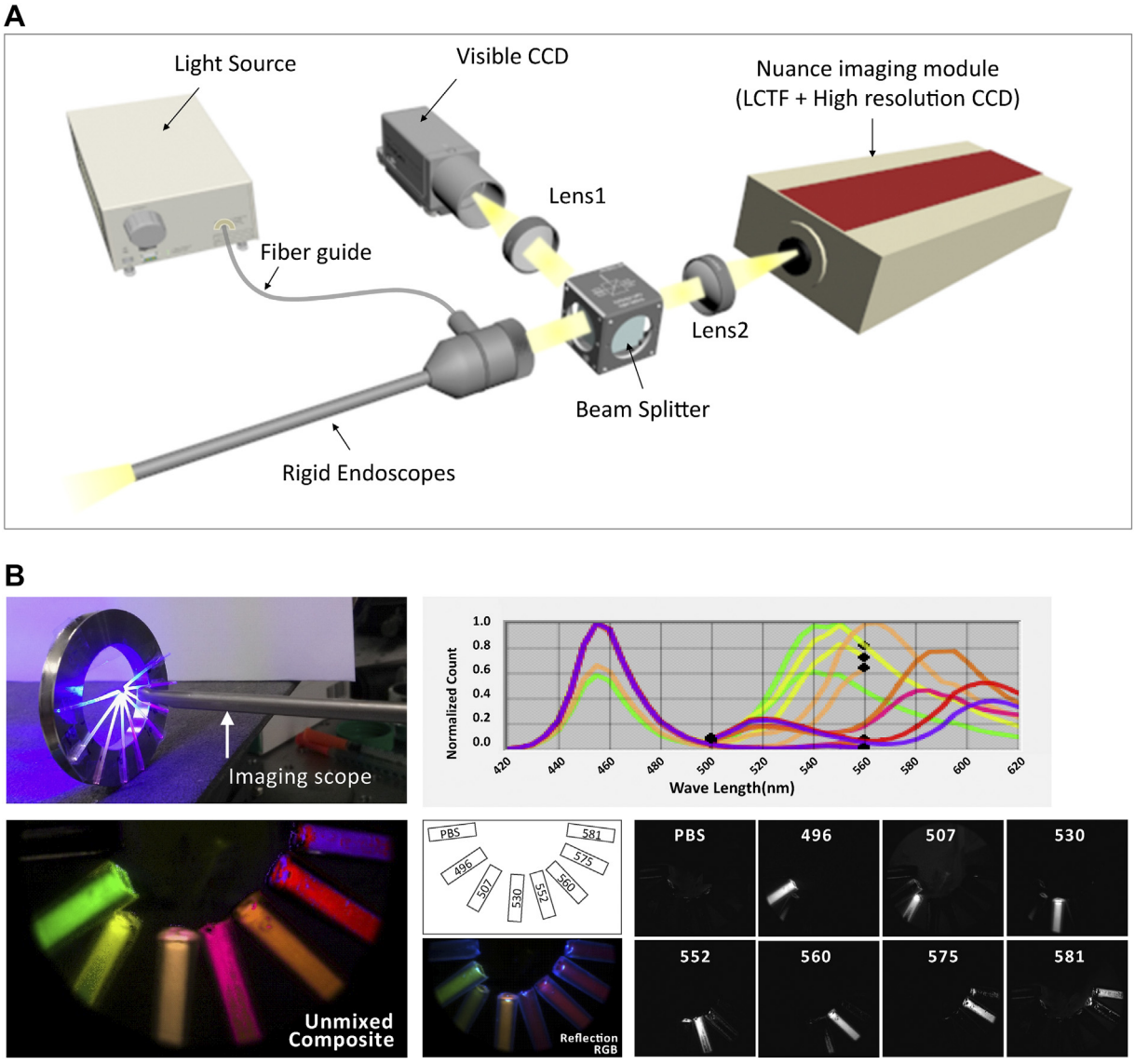

Figure 1. Setup of multi-spectral endoscope and phantom study. (A) Design and fabrication of multi-spectral endoscope. Detection of white light image was performed by CCD camera and fluorescent image by Nuance camera. The collected images or fluorescence signal is divided in beam splitter and passes through each lens in front of two CCD camera. The excitation light which is generated from xenon lamp goes into endoscopic channel and excites fluorophores of fluorescent probes. (B) Demonstration of multiplexing on phantom study with a polyethylene mock-up tube, which was attached to metal ring (Left upper). (Lower) Each unmixed signal is seen with (Left lower) and without (Right lower) pseudo-color. The bare-eyed reflection image is shown in the figure (Reflection RGB, middle lower). The graph represents emission spectra of each dyes (Upper Right).

a very narrow band-pass (± 5 to 20 nm) and wavelength tuning element. Nuance acquisition software (PerkinElmer, Hopkinton, MA) was developed along with the imaging system to capture and analyze the multi-spectral images.

The sample exposure time for the Nuance camera was adjusted from 200 ms to 800 ms depending on the sample brightness. A series of fluorescence images at different wavelengths were rapidly acquired by the Nuance CCD camera and the data was assembled into a spectral data "cube" for analyzing fluorescence spectra in a few seconds.

Spectral Unmixing, Autofluorescence Elimination And Imaging Analysis

For the spectral unmixing in the inspected tissues, we established a "Spectral Library" using negative and positive control subjects. Acquiring the Spectral Library was as follows: 1) Selecting cube wavelengths for emission scan for the fluorescent probes, 2) Determining optimal exposure time for the subject to observation adjusting exposure time so as not to saturate (below 60,000 counts), 3) Acquiring one "ImageCube" after sequentially taking multispectral image stacks from the emission planes which are collected according to excitation light, and 4) Creating a Spectral Libraries in a file from negative and positive control groups. Spectral unmixing is executed with sophisticated algorithms (RCA: real component analysis) of Nuance software. Then the targeted fluorophores from administered probes can be separated from every component in the acquisition through the use of spectral subtraction and negative controls. Using the morphologic segmentation analysis software "inForm" (PerkinElmer), the positive area of fluorescence signal in polyp was segmented and analyzed. The software was trained to recognize polyp area

with "Trainable Tissue Segmentation" in the software and scored the percentage of the occupied fluorescence signal.

Phantom Study

Phantom study was performed with a polyethylene (PE-10) mock-up tube (15 mm long, 0.28 mm inner diameter), which was attached to metal ring (Figure 1*B*). Each polyethylene tube was filled with fluorescent dye solutions that has broad range of fluorescence spectra, and measured in the range from 420 nm to 620 nm with 5 nm step. The fluorescent dyes used here were as following: Flamma-496 (Ex/Em 496/516 nm), Flamma-507 (Ex/Em 507/532 nm), Flamma-530 (Ex/Em 530/558 nm), Flamma-553 (Ex/Em 554/584 nm), Flamma-560 (Ex/Em 560/589 nm), Flamma-575 (Ex/Em 578/606 nm) and Flamma-581 (Ex/Em 578/595 nm). Multiple fluorophores was sequentially excited with blue excitation (480 nm) and green excitation (525 nm) from LED light source (TouchBrightLED, Seoul, South Korea) under the exposure time condition of 900 ms in the emission range of 420 nm to 530 nm and 500 ms in the emission

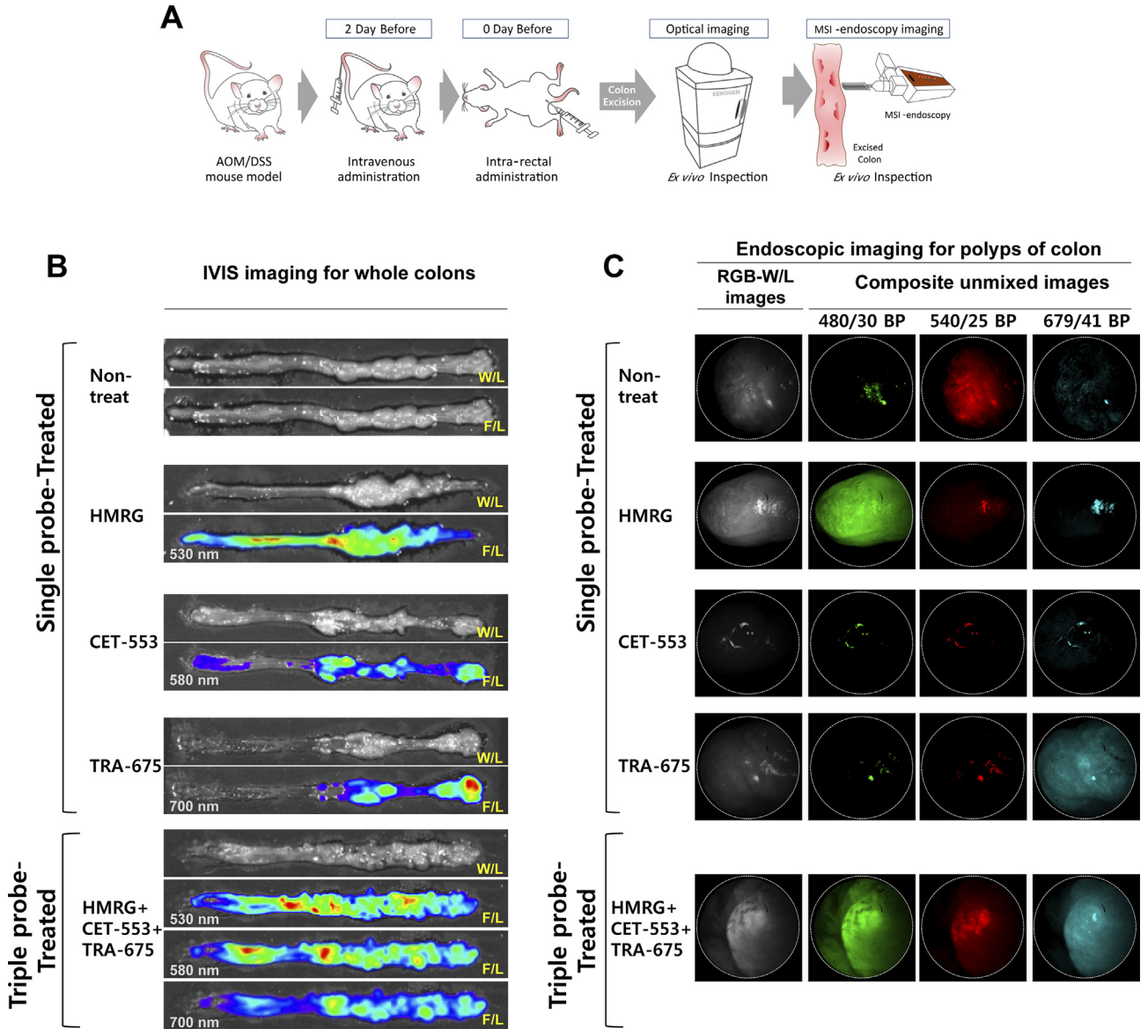

Figure 2. *Ex vivo* colon tissue imaging with multispectral endoscope and IVIS system. (A) An illustrated flow showing the performed *ex vivo* experiments. Mouse is administered with fluorescence probes and examined by optical instrument and MSI-endoscopy. Individually targeted *ex vivo* colon polyp images from mouse treating with single probe only and triple probes simultaneously. Excised colons were scanned for IVIS wide-field fluorescence imaging (B) and imaged with multi-spectral fluorescence endoscope system (C). The whole view of white-light (W/L) and IVIS optical fluorescence-light (F/L) imaging of colon is shown (B). Apply of two antibodies (i.v.) and HMRG (spraying) sequentially results in separate spatial patterns of binding to colonic dysplasia. The wavelength of emission planes is as follows: 520–560 nm (five planes, 10 nm scan step), 600–640 nm (five planes, 10 nm scan step) and 690–720 nm (four planes, 10 nm scan step). The composite unmixed images of single-probe-treated polyp showed respective signal under the excitation with band-pass filter of 480/30 nm for green, 540/25 nm for red and 679/41 nm for skyblue pseudocolor and triple-probe-treated polyp showed all positive signal under all excitation light.

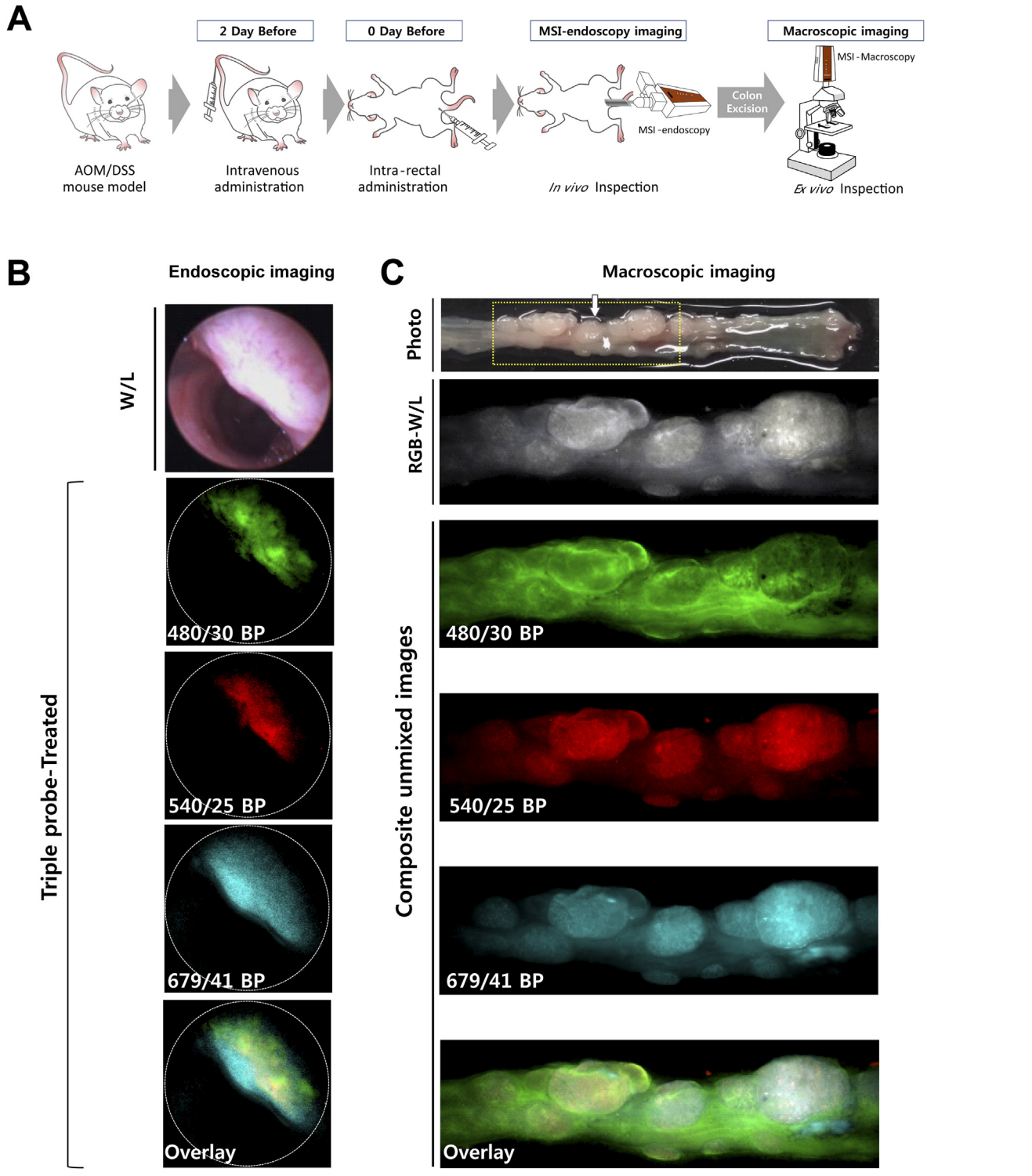

Figure 3. *In vivo* real-time multispectral endoscopic imaging and *ex vivo* imaging. (A) An illustrated flow showing the performed in real-time *in vivo* and *ex vivo* experiments. Mouse is administered with fluorescence probes and examined by multi-spectral endoscopy and macroscopy. (B) *In vivo* fluorescence image of polyps using separately administered probes gGlu-HMRG (HMRG), Cetuximab (CET-553) and Trastuzumab (TRA-675). The white light image of inspected polyp is shown at the end to the left. (C) The colon from fig. (B) was resected from the examined mouse and inspected with multi-spectral macroscopy. The whole view (Photo) and macroscopic monochrome image (Monochrome) of colon are shown in the top of column. The macroscopic fluorescence images show different patterns of signal at each spectrum. The white arrow indicates the inspected polyp shown *in vivo*.The composite unmixed images of single-probe-treated polyp showed respective signal under the excitation with band-pass filter of 480/30 nm for green, 540/25 nm for red and 679/41 nm for skyblue pseudocolor and triple-probe-treated polyp showed all positive signal under all excitation light. (D) Threshold segmentation of multiple fluorophores using inform software and positive area of fluorescence signal in polyp quantification. (E) H&E histology of polyp shows features similar to those seen in sporadic human adenomas. (F) Confocal microscopy images showing binding of fluorescence probe to colon tissue. Biopsies tissue were excised after *in vivo* administration of probes and images were collected. Untreated colon polyp was shown as control.

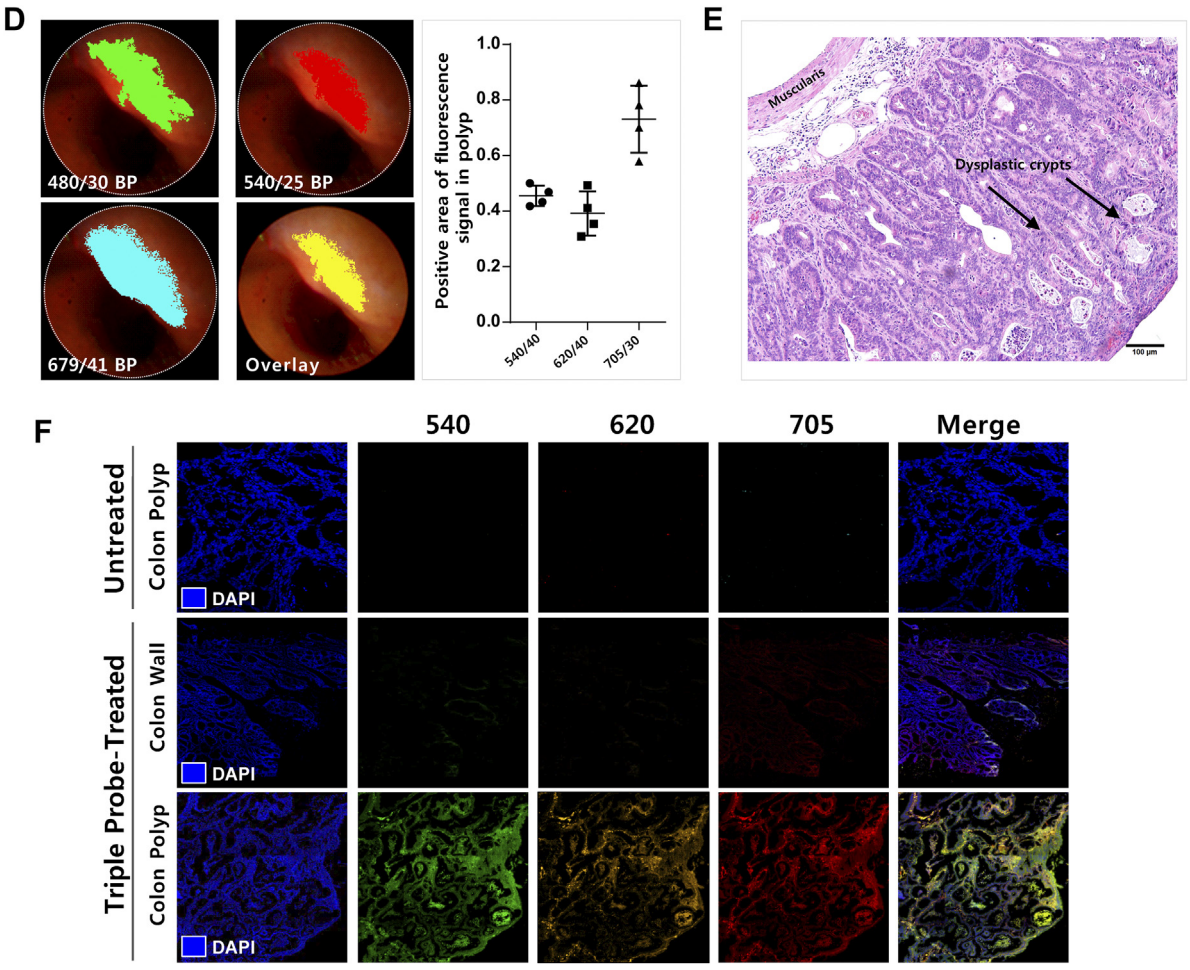

Figure 3 (*continued*).

range of 530 nm to 620 nm, respectively. The assembled spectral data were utilized to separate specific fluorescence labels over the tissue autofluorescence.

AOM/DSS Mouse Model of Polypoid Adenomas

Five-week-old male BALB/c mice were used for inflammation-driven colonic tumorigenesis utilizing a single injection of AOM followed by 2 seven-day cycles of DSS over a 8 week period.

Azoxymethane (AOM, 10 mg/kg body weight; Sigma–Aldrich, MO, USA) is intraperitoneally injected on day 0 and at the beginning of the second week (day 7), dextran sodium sulfate solution (DSS, 2%; MP Biomedicals, Illkirch, France) is administered to mice in their drinking water. Seven days of DSS is followed by 2 weeks of switching back a basal diet and tap water. Another additional 1 cycle of DSS are administered, and tumor formation in the colonic wall was examined with colonoscopy. All animal experiments were performed with protocols approved by the Institutional Animal Care and Use Committee (IACUC) of the Asan Institute for Life Sciences, Asan Medical Center. The committee abides by the Institute of Laboratory Animal Resources (ILAR) guide.

Preparation of Fluorescence Molecular Probes

We adopted monoclonal antibody cetuximab (Erbitux; Merck KGaA, Darmstadt, Germany) and trastuzumab (Herceptin; Roche, Basel, Switzerland) for its interaction with EGFR and HER2, respectively. An activatable probe, γ-glutamyl hydroxymethyl rhodamine green (gGlu-HMRG), is another agent to detect the cancerous lesions. This probe is rapidly activated by γ-glutamyltranspeptidase (GGT) which is over-expressed on the cell membrane of various cancer, but is not expressed in normal tissue [30,31].

gGlu-HMRG was prepared according to the synthesis of references [32] by BioActs (Incheon, Korea) and monoclonal antibodies were conjugated with fluorescent dyes (Flamma-553 NHS ester, Flamma-675 NHS ester, respectively) according to the company's protocol.

Endoscopic Imaging of Colon Ex Vivo And In Vivo

AOM/DSS mice model (age over 15 weeks old) were used for imaging. Conventional white light endoscopy was executed for screening and identifying the presence of polyps in the mice colon. Due to the pharmacodynamics of the antibody probe, it accumulates persistently in the target of the tumor and takes a certain amount of time to be released from surrounding normal tissue. We performed preliminarily a controlled experiment to determine the optimized time point for acquiring good target-to-background ratio by examining in experimental mice after injecting the antibody probe. The targeting probes (CET-553 and TRA-675) were administered in the mice *via* tail vein injection, 2 days before the endoscopic imaging. Mice were fasted over 8 hours, and stool in the colon was removed by a saline lavage for spaying of the activatable probe HMRG. The HMRG was intrarectally administrated by instilling with disposable

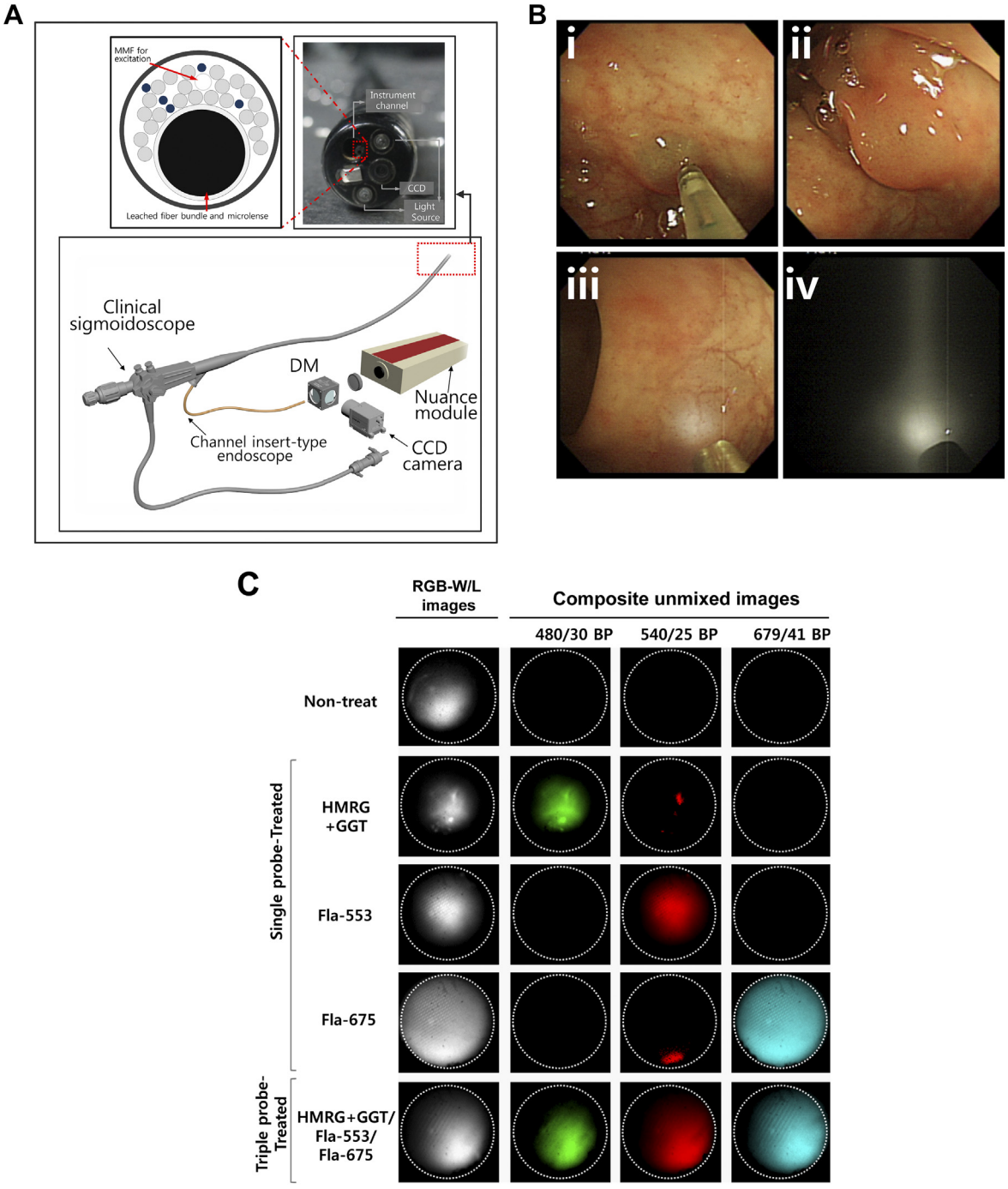

Figure 4. *In vivo* real-time multispectral endoscopic imaging with channel insert-type endoscope device in porcine. (A) Schematic of channel insert-type endoscope designed to be inserted through the accessory channel of a clinical sigmoidoscope with a 3.2-mm instrument channel. The enlarged frontal view of imaging scope (Upper left), distal end of sigmoidoscope (Upper right) and the whole view of channel insert-type endoscope (Lower) is presented (DM: Dichroic mirror, MMF: Multi-mode fiber). (B) White-light endoscopic screenshot of making pseudo polyp (i-ii) and illuminating on the colon wall of porcine in the state of white-light mode (iii) and fluorescence mode (iv). (C) Multi-spectral fluorescent imaging with fluorescent dye sample and unmixing imaging. The activated form of HMRG after mixed with GGT in advance, Flamma-553 and Flamma-675 dyes or/and all three mixed dye was infused onto the colon wall of porcine.The images represented that single dye-infused polyp showed respective signal under the excitation with band-pass filter of 480/30 nm for green, 540/25 nm for red and 679/41 nm for skyblue pseudocolor and triple-probe-treated polyp revealed all positive signal at all spectra. The last column to the left shows a monochrome image collected at 540 ± 40 for Non-treat and HMRG group, 620 ± 40 for CET-553 group and 705 ± 30 for TRA-675 group respectively.

zonde and incubated for 5 minutes. For *ex vivo* endoscopy, the colon was excised and incised to expose the lumen of colon. The colon tissue was laid down on a flat plate, and faced to the tip of small animal endoscope. For *in vivo* imaging, the mice were anesthetized by inhaling isoflurane gas mixed with oxygen, and the colon was insufflated with CO_2 gas. The colon was monitored through the CCD camera and the multi-spectral imaging was conducted if polys were detected. Xenon lamp was used as a light source at designated

excitation wavelength with band-pass filters of 480/30 nm, 540/25 nm and 679/41 nm (Asahi Spectra, Torrance, CA). The individual excitation for emission planes of "ImageCube" is as follows: 480/30 BP excitation with five planes (520, 530, 540, 550 and 560 nm), 540/25 BP excitation five planes (600, 610, 620, 630 and 640 nm) and 679/41 BP with four planes (690, 700, 710 and 720 nm).

Ex Vivo Fluorescence Optical and Macroscopic Imaging

The excised colon tissues were then moved into the IVIS Spectrum system (PerkinElmer, Hopkinton, MA) and the fluorescence signal was collected. The excitation/emission wavelengths for HMRG, CET-553 and TRA-675 were 465/520 nm, 554/584 nm and 675/691 nm, respectively under auto acquisition setup. For macroscopic inspection, Nuance was attached to the MacroFluo Z16 APO macroscope (Leica) and operated by the Nuance software.

Imaging with Channel Insert-Type Endoscope System for Multi-Spectral Fluorescent Imaging

Specific details of the channel insert-type endoscope system are described in the literature [33] and schematic is shown in Figure 4*A*. Briefly, the device is fabricated with flexible and miniaturized fiber-optic probe for the compatibility with clinical endoscope in non-contact mode. The imaging scope consists of a micro lens attached to a leached fiber bundle and multimode fibers (NA 0.55, SCHOTT AG) for delivering excitation light using an achromatic VIS–NIR-coated lens with an effective focal length (EFL) of 18 mm. Excitation light was delivered from the same xenon lamp used in rigid type endoscope of previous mouse studies and the fluorescence light from reflection and emission are collected *via* a micro-lens and relayed back to the optical path by the image scope. The light passes through two achromatic lenses with EFLs of 10 and 40 mm (Edmund Optics), LCTF of Nuance, and a dichroic mirror. The reflection image is captured by a CCD camera (QIClick, QImaging) and fluorescence images are acquired sequentially with scientific-grade CCD camera of Nuance. We demonstrated the multi-spectral fluorescent imaging of the channel insert-type endoscope both in the simulated dummy colon model and the porcine colon to validate sigmoidoscopic feasibility in the clinic. To mimic the polyp bearing accumulated fluorescent probes, we produced dye-agar droplets (2% agar, 5–6 mm size), which were made by mixing agar and each three fluorescent dyes (FITC, Flamma-553 and Flamma-675) and solidified as stiff gel. The dye-agar droplets were attached on the wall of dummy colon model and endoscopic imaging was performed.

For *in vivo* validation of channel insert-type endoscope system, we used a porcine colon of Yorkshire pig weighing 30 kg. The pig was anesthetized with 4% isoflurane for induction and maintained with 1.5 ± 2% by continuous inhalation through endotracheal intubation. We created pseudo polyps comprising the fluorescence dye onto the colon wall using a clinical injection needle (NM-400 U-0423, Olympus). Each fluorescent dye (2 mg/ml) and the activated form of HMRG (51 mU GGT+ 50uM HMRG) probes were individually injected to the polyps, or their mixture (300 μl) was simultaneously introduced. The animal studies were performed under the supervision of the IACUC of the Asan Medical Center by the approved institutional protocols.

Histological Evaluation

The localization of each fluorescent probe in resected colon tissues of mice, along with the morphology, were evaluated by histological analysis. Excised colon tissues of mice were fixed with 10% formalin, and 1) embedded in paraffin or 2) frozen in OCT medium, followed by section into slices. Paraffin-sectioned slices were stained with H&E using common procedure. Cryo-sectioned tissue slices were stained with 4,6-diamidino-2-phenylindole (DAPI) for nuclei, slide-mounted, and sealed. Samples were pictured by a conventional eclipse microscopy or a confocal microscopy (Carl Zeiss, Inc., Jena, Germany).

Results

The ability of multi-spectral endoscope device equipped with the Nuance camera was firstly performed with a phantom study as shown in Figure 1*B*. Polyethylene tubes filled with fluorescent dyes of different emission band edges were located at the end of telescope probe, and the emission spectra were simultaneously measured. To execute spectral unmixing, we obtained the intrinsic emission spectra of each dye, and then used as reference to separate the overlapped emission spectra (spectral unmixing). The pseudo color images of unmixed emission signals represent highly enhanced spectral difference of each fluorescent dye, compared to the reflection image shown in naked eye (Reflection RGB).

To assess the ability of multi-spectral fluorescence endoscope device to multiplex *ex vivo*, two probes (CET-553 and TRA-675) were two days before and one probe (HMRG) was just prior to mouse sacrifice administered (Figure 2*A*). The whole colon tissue was spread on a flat plate and investigated by the multi-spectral fluorescence endoscope. Figure 2*C* shows the representative fluorescence endoscopic images of the colon tissues, in which each targeting probe have been introduced. Polypoid lesion of non-treated group at the first row in Figure 2*C* showed specular reflection from surface of dysplasia and seen as a false positive signal due to the close distance between the dampish tissue of colon polyps and the end of the telescope.

However, specific fluorescence signals were detected in the targeting probe-treated groups: HMRG at 540/40, CET-553 at 620/40 and TRA-675 at 705/30. The results support that each targeting probe enabled to home the cancerous lesion in the colon, and the fluorescence signal of each probe was clearly distinguishable in different emission band. These spectra information were collected as a spectrum library, and accordingly used as a reference for spectral unmixing in the following validation. We next applied three targeting probes simultaneously. The fluorescence images revealed positive signals for all targeting probes, suggesting that three probes have certain specific interactions with the polyps. Interestingly, the targeted areas of each probe showed slightly different shape, particularly in CET-553, possibly due to variation of the receptors overexpressed even in a cancerous polyp. The cetuximab-positive epidermal growth factor receptor (EGFR) seemed to be slowly overexpressed than the trastuzumab-positive HER2, otherwise there was difference in the targeting efficacy between cetuximab and trastuzumab at one polyp. To verify the multi-spectral targeting, we then imaged the whole colon with a conventional fluorescence imaging system, IVIS (Figure 2*B*). The antibody-treated mice showed significant fluorescence signals at the polypoid lesion of the colon while negligible in the normal colon. However, since there is variation from differences between individual mice and number of polyps in a mouse colon, the comparison of fluorescence intensity at the polypoid lesion between each probe treatment group is not significant. The results clearly support the targeting specificity of cetuximab and trastuzumab to the lesions. The activatable probe showed strong fluorescence signals at both polypoid lesions and the margins between polyps of adjacent normal mucosa. Especially, it will not be irrelevant to the characteristics of spray-type probe that

some of the remaining HMRG probes appear as a partial accumulation in the margin area.

We next demonstrated *in vivo* endoscopic imaging from the colon of AOM/DSS mouse model. Administration of three fluorescence probes was carried out in advance in the same way as *ex vivo* experiment (Figure 3*A*). We obtained the images of colon using the multi-spectral fluorescence endoscopy system in the single probe-treated group (Supplementary Figure S1), and then used the spectral information as a spectral library data for unmixing process of multiple fluorescence signals. The fluorescence images of live mice colon also showed clearly distinguishable lesions *via* fluorescence signals (Figure 3*B*). Corresponding to the *ex vivo* study, the multiple targeting probes designated the fluorescent lesions over normal colon tissue. Acquired fluorescence spectra were sufficiently separated by unmixing in the Nuance software. To validate the fluorescence signals on polyps of colon in macroscopic view, we facilitated the Nuance camera module with macroscopy and imaged the corresponding colon tissue after sacrifice of mice (Figure 3*C*). In the i.v.-administered Ab group, a strong signal was seen in the polyp, and in the spraying-administered HMRG group, the signal was seen not only in the polyp but also in the adjacent normal mucosa of colon wall. The macroscopic imaging of the single probe-treated group was performed (Supplementary Figure S2). The images showed distinct fluorescence at the lesions, corresponding to the above results. In addition, we designated the regions of interest (ROI) for the target-signal (Ts) and the whole polyp (Tp), and then calculated the positive area of fluorescence signal in polyp. Using the inform analysis, we obtained the positive area of fluorescence signal in polyp that appeared as segmentation and the Ts/Tp ratio: 0.46 ± 0.04 (HMRG), 0.39 ± 0.08 (CET-553) and 0.73 ± 0.12 (TRA-675), respectively (Figure 3*D*). This segmentation and quantification of target-intensity may allow the clinician to determine the type and dosage of medicine to apply to the patient for follow up treatment. The corresponding lesion was evaluated with histology (hematoxylin and eosin (H&E) staining) and showed dysplasia, characterized by crypt distortion and nuclear enlargement (Figure 3*E*). Confocal microscopy images of biopsied tissue collected subsequent to probe administration represented that the probe signal was mostly appeared on probe-treated polyp, but not on probe-treated adjacent colon wall and probe-untreated polyp (Figure 3*F*). To validate the fluorescence signal, we scanned the whole colon of single and triple probe-treated group with IVIS wide-field fluorescence imaging system (Supplementary Figure S3).

For the clinical application of multi-spectral fluorescent endoscopy system, the channel insert-type endoscope was equipped with the sigmoidoscope (Figure 4*A*). The imaging system was connected to the Nuance module, and applied to simulated dummy colon model (Supplementary Figure S4) and the porcine colon (Figure 4*B*) to investigate the clinical suitability with the sigmoidoscope. A video showing real-time imaging of performance for the multi-spectral fluorescence endoscopic system with the channel insert-type endoscope is provided in Supplementary Video 1. The end of channel insert-type endoscope is shown to approach near to the dye-agar droplets on the wall of simulated dummy model. The last video segment shows the conversion of imaging mode from white light to fluorescence flashing dye-agar droplets.

Finally, we adopted the imaging system for tumor surveillance in the pseudo polyp on the colon wall of porcine model where the fluorescent probes were infused on purpose (Figure 4*B* (i-ii)). Multi-spectral fluorescent imaging was then performed, and showed clearly distinguishable area of the probe infusion (Figure 4*B* (iii-iv)). White light video in Supplementary Video 2 is shown for the real-time imaging of producing blister-like pseudo polyps by injection of fluorophores. The fluorescence signals of HMRG mixed with GGT, Flamma-553 and Flamma-675 dyes showed well-defined spectral unmixing in the present system, and their mixture was also simultaneously displayed with the respective signal at the corresponding emission peak band (Figure 4*C*).

Discussion

Here, we report a multi-spectral fluorescent endoscopy system that can clearly separate multiple fluorescent spectra probes to visualize the individual probe *via* spectral unmixing. The fluorescent probes were introduced both systemically and topically to the mouse colon, followed by imaging *in vivo* and *ex vivo*. To achieve this multi-spectral fluorescent imaging, the emission spectra need to be appropriately separated one-by-one, thus an endoscopic device to unmix various fluorescent probes is a key demand. The required specifications are likely to fulfill the capabilities of unmixing different emission spectrum of each probe and eliminating intrinsic autofluorescence which distracts the probe signals particularly in the gastrointestinal tract [9].

We performed multi-spectral endoscopic imaging for the polyps *ex vivo* and *in vivo*, accompanied by conventional fluorescence imaging instrument for macroscopic point of view. Specific targeting of each fluorescent probe was confirmed by clear distinction *via* spectral unmixing. In the future, this technology will enable to visualize tumor heterogeneity for understanding the tumor characters including anticancer drug responsiveness.

In addition, the multi-spectral imaging system can be used for monitoring clonal evolution of individual progenitors. The system can examine unique spatial patterns of gene overexpression by differentiating individual target gene, and provide a potential tool for studying epigenetic and environmental factors that influence cancer formation. This can be further applied to perform personalized image-guided therapy. While three channels were executed in the present study, the optical design can be adapted for using more fluorescent dyes, as we showed very sensitive spectral unmixing in the visible to near-infrared regime (Figure 1*B*). Present study is the first report on an endoscope-compatible instrument that can concurrently image multiple molecular probes in different spectral regimes over the usage mostly in the field of conventional microscopy.

Endoscopic imaging of mouse colon has been performed with rigid-type small animal endoscope, however we developed the multi-spectral imaging system, compatible to flexible channel insert-type endoscope for clinical use as a translational medical device. The flexible fluorescence endoscopic system can be applied for molecular diagnosis along with conventional white-light colonoscopy to identify flat dysplasia lesions.

Our system, on the other hand, has a limitation related to low transmission for fluorescence emission light of LCTF which is typically 30%-range compared to conventional filters (~90%) [34]. Low transmittance results in relatively the drawback of requiring long exposure times for acquiring image.

However, LCTF has great capability of using multiple filters rapidly with fast movement between filters, resulting in remarkable signal-to-noise ratio through the spectral unmixing process. Therefore, it is expected that problems will be overcome if the LCTF which has the disadvantage of transmittance is substituted for a single filter

and a conventional filter system which has the disadvantage of switching between filters is substituted for a high-speed filter wheel. We are developing the multi-spectral fluorescence endoscope with high performance filter wheel bearing unmixing algorithm, thus this will lead to improved early cancer detection for appropriate treatments for patient.

Supplementary data to this article can be found online at https://doi.org/10.1016/j.tranon.2018.10.006.

Acknowledgements

The authors thank Alexay V. Dan Chin-Yu in Hyunjoo In-Tech for his technical support in channel insert-type endoscope system, Dr. Joon Seo Lim from the Scientific Publications Team at Asan Medical Center for his editorial assistance in preparing this manuscript, BioActs for their support in synthesizing gGlu-HMRG and also thank the optical imaging core facility at the ConveRgence mEDIcine research cenTer (CREDIT), Asan Medical Center for support and instrumentation.

References

[1] Siegel RL, Miller KD, and Jemal A (2016). Cancer statistics, 2016. *CA Cancer J Clin* **66**, 7–30.

[2] Cunningham D, Atkin W, Lenz HJ, Lynch HT, Minsky B, Nordlinger B, and Starling N (2010). Colorectal cancer. *Lancet* **375**, 1030–1047.

[3] Zauber AG, Winawer SJ, O'Brien MJ, Lansdorp-Vogelaar I, van Ballegooijen M, Hankey BF, Shi W, Bond JH, Schapiro M, and Panish JF, et al (2012). Colonoscopic polypectomy and long-term prevention of colorectal-cancer deaths. *N Engl J Med* **366**, 687–696.

[4] Hart AR, Kudo S, Mackay EH, Mayberry JF, and Atkin WS (1998). Flat adenomas exist in asymptomatic people: important implications for colorectal cancer screening programmes. *Gut* **43**, 229–231.

[5] Hurlstone DP, Cross SS, Adam I, Shorthouse AJ, Brown S, Sanders DS, and Lobo AJ (2003). A prospective clinicopathological and endoscopic evaluation of flat and depressed colorectal lesions in the United Kingdom. *Am J Gastroenterol* **98**, 2543–2549.

[6] Kudo S, Kashida H, Tamura T, Kogure E, Imai Y, Yamano H, and Hart AR (2000). Colonoscopic diagnosis and management of nonpolypoid early colorectal cancer. *World J Surg* **24**, 1081–1090.

[7] Judge TA, Lewis JD, and Lichtenstein GR (2002). Colonic dysplasia and cancer in inflammatory bowel disease. *Gastrointest Endosc Clin N Am* **12**, 495–523.

[8] Yang C, Hou VW, Girard EJ, Nelson LY, and Seibel EJ (2014). Target-to-background enhancement in multispectral endoscopy with background autofluorescence mitigation for quantitative molecular imaging. *J Biomed Opt* **19**76014.

[9] Mansfield JR, Gossage KW, Hoyt CC, and Levenson RM (2005). Autofluorescence removal, multiplexing, and automated analysis methods for in-vivo fluorescence imaging. *J Biomed Opt* **10**41207.

[10] Zavaleta CL, Garai E, Liu JT, Sensarn S, Mandella MJ, Van de Sompel D, Friedland S, Van Dam J, Contag CH, and Gambhir SS (2013). A Raman-based endoscopic strategy for multiplexed molecular imaging. *Proc Natl Acad Sci U S A* **110**, E2288-2297.

[11] Goetz M and Wang TD (2010). Molecular imaging in gastrointestinal endoscopy. *Gastroenterology* **138** [828-833.e821].

[12] Liu Z, Miller SJ, Joshi BP, and Wang TD (2013). In vivo targeting of colonic dysplasia on fluorescence endoscopy with near-infrared octapeptide. *Gut* **62**, 395–403.

[13] Hazewinkel Y, Lopez-Ceron M, East JE, Rastogi A, Pellise M, Nakajima T, van Eeden S, Tytgat KM, Fockens P, and Dekker E (2013). Endoscopic features of sessile serrated adenomas: validation by international experts using high-resolution white-light endoscopy and narrow-band imaging. *Gastrointest Endosc* **77**, 916–924.

[14] Yamada M, Sakamoto T, Otake Y, Nakajima T, Kuchiba A, Taniguchi H, Sekine S, Kushima R, Ramberan H, and Parra-Blanco A, et al (2015). Investigating endoscopic features of sessile serrated adenomas/polyps by using narrow-band imaging with optical magnification. *Gastrointest Endosc* **82**, 108–117.

[15] Boparai KS, van den Broek FJ, van Eeden S, Fockens P, and Dekker E (2009). Hyperplastic polyposis syndrome: a pilot study for the differentiation of polyps by using high-resolution endoscopy, autofluorescence imaging, and narrow-band imaging. *Gastrointest Endosc* **70**, 947–955.

[16] Weissleder R (2006). Molecular imaging in cancer. *Science* **312**, 1168–1171.

[17] Miller SJ, Lee CM, Joshi BP, Gaustad A, Seibel EJ, and Wang TD (2012). Targeted detection of murine colonic dysplasia in vivo with flexible multispectral scanning fiber endoscopy. *J Biomed Opt* **17**021103.

[18] Burggraaf J, Kamerling IM, Gordon PB, Schrier L, de Kam ML, Kales AJ, Bendiksen R, Indrevoll B, Bjerke RM, and Moestue SA, et al (2015). Detection of colorectal polyps in humans using an intravenously administered fluorescent peptide targeted against c-Met. *Nat Med* **21**, 955–961.

[19] Zhou L and El-Deiry WS (2009). Multispectral fluorescence imaging. *J Nucl Med* **50**, 1563–1566.

[20] Levenson RM, Lynch DT, Kobayashi H, Backer JM, and Backer MV (2008). Multiplexing with multispectral imaging: from mice to microscopy. *ILAR J* **49**, 78–88.

[21] Yang C, Hou V, Nelson LY, and Seibel EJ (2013). Mitigating fluorescence spectral overlap in wide-field endoscopic imaging. *J Biomed Opt* **18**86012.

[22] Misale S, Bozic I, Tong J, Peraza-Penton A, Lallo A, Baldi F, Lin KH, Truini M, Trusolino L, and Bertotti A, et al (2015). Vertical suppression of the EGFR pathway prevents onset of resistance in colorectal cancers. *Nat Commun* **6**, 8305.

[23] Prahallad A, Sun C, Huang S, Di Nicolantonio F, Salazar R, Zecchin D, Beijersbergen RL, Bardelli A, and Bernards R (2012). Unresponsiveness of colon cancer to BRAF(V600E) inhibition through feedback activation of EGFR. *Nature* **483**, 100–103.

[24] Misale S, Yaeger R, Hobor S, Scala E, Janakiraman M, Liska D, Valtorta E, Schiavo R, Buscarino M, and Siravegna G, et al (2012). Emergence of KRAS mutations and acquired resistance to anti-EGFR therapy in colorectal cancer. *Nature* **486**, 532–536.

[25] Qian X, Peng XH, Ansari DO, Yin-Goen Q, Chen GZ, Shin DM, Yang L, Young AN, Wang MD, and Nie S (2008). In vivo tumor targeting and spectroscopic detection with surface-enhanced Raman nanoparticle tags. *Nat Biotechnol* **26**, 83–90.

[26] Siravegna G, Mussolin B, Buscarino M, Corti G, Cassingena A, Crisafulli G, Ponzetti A, Cremolini C, Amatu A, and Lauricella C, et al (2015). Clonal evolution and resistance to EGFR blockade in the blood of colorectal cancer patients. *Nat Med* **21**, 827.

[27] Ingold Heppner B, Behrens HM, Balschun K, Haag J, Kruger S, Becker T, and Rocken C (2014). HER2/neu testing in primary colorectal carcinoma. *Br J Cancer* **111**, 1977–1984.

[28] Valtorta E, Martino C, Sartore-Bianchi A, Penaullt-Llorca F, Viale G, Risio M, Rugge M, Grigioni W, Bencardino K, and Lonardi S, et al (2015). Assessment of a HER2 scoring system for colorectal cancer: results from a validation study. *Mod Pathol* **28**, 1481–1491.

[29] Jordan NV, Bardia A, Wittner BS, Benes C, Ligorio M, Zheng Y, Yu M, Sundaresan TK, Licausi JA, and Desai R, et al (2016). HER2 expression identifies dynamic functional states within circulating breast cancer cells. *Nature* **537**, 102–106.

[30] Urano Y, Sakabe M, Kosaka N, Ogawa M, Mitsunaga M, Asanuma D, Kamiya M, Young MR, Nagano T, and Choyke PL, et al (2011). Rapid cancer detection by topically spraying a gamma-glutamyltranspeptidase-activated fluorescent probe. *Sci Transl Med* **3**110ra119.

[31] Kamiya M, Kobayashi H, Hama Y, Koyama Y, Bernardo M, Nagano T, Choyke PL, and Urano Y (2007). An enzymatically activated fluorescence probe for targeted tumor imaging. *J Am Chem Soc* **129**, 3918–3929.

[32] Sakabe M, Asanuma D, Kamiya M, Iwatate RJ, Hanaoka K, Terai T, Nagano T, and Urano Y (2013). Rational design of highly sensitive fluorescence probes for protease and glycosidase based on precisely controlled spirocyclization. *J Am Chem Soc* **135**, 409–414.

[33] Oh G, Park Y, Yoo SW, Hwang S, Chin-Yu AV, Ryu YM, Kim SY, Do EJ, Kim KH, and Kim S, et al (2017). Clinically compatible flexible wide-field multi-color fluorescence endoscopy with a porcine colon model. *Biomed Opt Express* **8**, 764–775.

[34] Levenson RM and Mansfield JR (2006). Multispectral imaging in biology and medicine: slices of life. *Cytometry A* **69**, 748–758.